ADVANCES IN ATMOSPHERIC SCIENCES, VOL. 32, OCTOBER 2015, 1391–1406

Recent Changes in Precipitation Extremes in the Heihe River Basin, Northwest China

CHENG Aifang[1,2], FENG Qi*[1], Guobin FU[3], ZHANG Jiankai[4], LI Zongxing[1,2], HU Meng[5], and WANG Gang[1,2]

[1]*Cold and Arid Regions Environmental and Engineering Research Institute, Chinese Academy of Sciences, Lanzhou* 730000
[2]*University of Chinese Academy of Sciences, Beijing* 100049
[3]*CSIRO Land and Water Flagship, Private Bag 5, Wembley WA* 6913*, Australia*
[4]*School of Atmospheric Sciences, Lanzhou University, Lanzhou* 730000
[5]*Guangzhou Meteorological Satellite Ground Station, Guangzhou* 510640

(Received 12 September 2014; revised 30 March 2015; accepted 1 April 2015)

ABSTRACT

Changes in rainfall extremes pose a serious and additional threat to water resources planning and management, natural and artificial oasis stability, and sustainable development in the fragile ecosystems of arid inland river basins. In this study, the trend and temporal variation of extreme precipitation are analyzed using daily precipitation datasets at 11 stations over the arid inland Heihe River basin in Northwest China from 1960 to 2011. Eight indices of extreme precipitation are studied. The results show statistically significant and large-magnitude increasing and decreasing trends for most indices, primarily in the Qilian Mountains and eastern Hexi Corridor. More frequent and intense rainfall extremes have occurred in the southern part of the desert area than in the northern portion. In general, the temporal variation in precipitation extremes has changed throughout the basin. Wet day precipitation and heavy precipitation days show statistically significant linear increasing trends and step changes in the Qilian Mountains and Hexi Corridor. Consecutive dry days have decreased obviously in the region in most years after approximately the late 1980s, but meanwhile very long dry spells have increased, especially in the Hexi Corridor. The probability density function indicates that very long wet spells have increased in the Qilian Mountains. The East Asian summer monsoon index and western Pacific subtropical high intensity index possess strong and significant negative and positive correlations with rainfall extremes, respectively. Changes in land surface characteristics and the increase in water vapor in the wet season have also contributed to the changes in precipitation extremes over the river basin.

Key words: precipitation extremes, atmospheric circulation, Heihe River basin, Northwest China

Citation: Cheng, A. F., Q. Feng, G. B. Fu, J. K. Zhang, Z. X. Li, M. Hu, and G. Wang, 2015: Recent changes in precipitation extremes in the Heihe River basin, Northwest China. *Adv. Atmos. Sci.*, **32**(10), 1391–1406, doi: 10.1007/s00376-015-4199-3.

1. Introduction

Given their potentially severe impacts, as emphasized by the Intergovernmental Panel on Climate Change (IPCC) in their Special Report on Extremes (IPCC, 2012), extreme climate events and their changes are of particular relevance to society and natural systems. The changes, causes and mechanisms of temperature and precipitation extremes have been studied on regional and global scales (Frich et al., 2002; Aguilar et al., 2005; Zhai et al., 2005; Alexander et al., 2006; Klein Tank et al., 2006; Nandintsetseg et al., 2007; Brown et al., 2008; Peterson et al., 2008; Choi et al., 2009; Fu et al., 2010; Vincent et al., 2011; Donat et al., 2013). These studies have revealed significant and widespread changes in temperature extremes consistent with warming, but less spatial coherence in precipitation extremes. Under global warming, magnitudes and patterns of extreme precipitation are expected to change (Trenberth et al., 2003; Groisman et al., 2005). However, compared with temperature, the characteristics, simulation, projected changes, and factors influencing precipitation extremes are more complex and uncertain, and vary greatly with region (Kiktev et al., 2007; Williams and Kniveton, 2012; Kunkel et al., 2012; van Pelt et al., 2012; Sillmann et al., 2013a, 2013b). Regional precipitation extremes occur when climate variability imposes large anomalies on the average state of the climate system (Pal and Al-Tabbaa, 2011). Extreme precipitation at smaller scales often has the greatest impacts (Knapp et al., 2008; Heisler-white et al., 2009; Samuels et al., 2009; Grant et al., 2010; Hossain et al., 2010; Rosenberg et al., 2010; Chiang and Chang, 2011; Marengo et al., 2012; Ran et al., 2012; Gregersen et al., 2013). However, features of extreme precipitation at larger (e.g., regional) scales may not reflect those at smaller scales. This is because what is considered an extreme in one part of a region might not be the case in another (Manton et al.,

* Corresponding author: FENG Qi
Email: qifeng@lzb.ac.cn

2001). Therefore, a detailed understanding is essential regarding changes in the frequency, duration, intensity, and spatial and temporal variability of precipitation extremes, as well as the causes, at smaller (e.g., local) scales.

Rainfall in areas west of 102.5°E in Northwest China has increased significantly, with the maximum linear trend reaching 0.15% $(10\ \mathrm{yr})^{-1}$ and exceeding the 95% confidence level in central Xinjiang and the eastern part of the Tibetan Plateau; while in areas east of that meridian, rainfall has declined (Yin, 2006). Several studies have addressed whether precipitation extremes have changed in accordance with variations in average precipitation. Wang and Zhou (2005) found that annual mean precipitation has increased significantly in most of Northwest China in all seasons, but daily precipitation extremes show increasing trends only in summer. Zhai et al. (2005) demonstrated a precipitation increase in terms of both intensity and frequency, and significant increases in extreme precipitation have been found in western China. You et al. (2011) investigated the spatiotemporal distributions of climate extreme indices during 1961–2003. They found that all extreme precipitation indices in Northwest China possess the largest positive trend magnitudes relative to other regions, and average wet day precipitation (PRCPTOT), maximum 1-day (R×1day) and 5-day (R×5day) precipitation amount, and heavy precipitation days show increasing trends; a decreasing trend was discovered for consecutive dry days (CDD), detailed descriptions of the indices are provided in Table 1. Wang et al. (2013) assessed extreme precipitation in arid areas of Northwest China and found that most precipitation extreme indices had increasing trends. The medians of precipitation indices showed insignificant change, except for CDD around 1986. Zhang et al. (2011a) reported that the number and total precipitation of maximum consecutive wet days (CWD) increased annually and in winter, implying a wet tendency in that season and in Northwest China. Afterward, based on a copula method, a modified Mann–Kendall trend test and linear regression, the spatiotemporal changes in precipitation indices in China were assessed over the period 1960–2005. Results indicated that regions west of 100°E, particularly Northwest China, had a wet tendency, reflected by increasing/decreasing numbers of consecutive rain/non-rain days (Zhang et al., 2013). Fu et al. (2013) indicated that Northwest China experienced an increasing trend of extreme rainfall events defined by duration and recurrence interval. Wang et al. (2012) reported significant increases in the number of rain days, simple daily intensity index (SDII), number of heavy precipitation days (R10), very wet days, R×1day and R×5day. CDD showed the opposite trend.

Precipitation and its extremes usually show no consistent trends in Northwest China as they are easily affected by the complex terrain and regional climate. Feng et al. (2014) found that high-intensity precipitation after drought was more than that under normal conditions over the entire Heihe River region. Li et al. (2014) indicated that extreme precipitation events were more intense after the 1990s and their occurrence was more frequent in the lower reaches of the river than in other parts. Zhang et al. (2015) reported that annual precipitation showed a significant increasing trend in the upstream part of the Heihe River, while no trends were detected for the middle and lower reaches of the river. The most notable period of increase for annual precipitation over the river was from 1977 to 1986 (Wang et al., 2010). Precipitation observed in the 1990s over the Heihe River has the largest range of variation, as compared with other decades in the past 50 years (Zhang et al., 2003). Much of the research on climate change in the Heihe River basin has concentrated on average precipitation series. However, there are limitations to using comprehensive indices to analyze extreme precipitation in the Heihe River basin, the second largest inland river basin in Northwest China.

Based on eight extreme precipitation indices and observed daily precipitation data, we analyze the characteristics of precipitation extremes across the Heihe basin during 1960–2011. The objectives are to (1) examine the spatial distribution of the general trends in extreme precipitation indices; (2) investigate the temporal variations and then evaluate the changes in the probability density function (PDF) of the detected precipitation extremes in various epochs and in each geographic unit of the basin; and (3) study the linkage between changes in extreme precipitation in the epochs and large-scale atmospheric circulation.

Table 1. Definitions of the extreme precipitation indices used in this study.

Index	Descriptive name	Definition	Units
CDD	Consecutive dry days	Maximum number of consecutive days with RR (daily precipitation) <1 mm in a year	d
CWD	Consecutive wet days	Maximum number of consecutive days with RR $\geqslant 1$ mm in a year	d
R10	Number of heavy precipitation days	Annual count of days when RR $\geqslant 10$ mm	d
SDII	Simple daily intensity index	Annual total precipitation divided by the number of wet days (defined as RR $\geqslant 1$ mm) in the year	mm d^{-1}
R95p	Very wet day precipitation	Annual total precipitation when RR $>$ 95th percentile of 1961–1990 daily rainfall	mm
PRCPTOT	Wet day precipitation	Annual total precipitation in wet days (RR $\geqslant 1$ mm)	mm
R×1day	Maximum 1-day precipitation amount	Annual maximum 1-day precipitation	mm
R×5day	Maximum consecutive 5-day precipitation amount	Annual maximum consecutive 5-day precipitation	mm

2. Study area

The Heihe River basin (Fig. 1) is a typical inland river basin in the arid zone of Northwest China (Cheng et al., 2014). It is located at the climatic intersection between the westerlies and the East Asian summer monsoon and has strong spatial heterogeneity with diverse ecosystems including an ice–snow zone, frozen soil, mountain forest, oasis, desert, and desert riparian forest (Kang et al., 2005; Qin et al., 2010). The river originates in the Qilian Mountains, which represents a water resource source area for the whole river and flows through a midstream region of irrigated agriculture, finally terminating at two lakes in the desert.

The upper stream is in the middle part of the Qilian Mountains, with high precipitation, low evaporation and temperature. The altitude range is 2000–5600 m and annual mean precipitation is 200–700 mm; potential evapotranspiration is about 700 mm (Ma and Frank, 2006). The middle stream is in the Hexi Corridor, where precipitation is low and evaporation high. Annual precipitation varies from 250 mm in the southern mountain area to less than 100 mm in the northern high plain area. The potential evapotranspiration is about 2000–2500 mm yr^{-1} and the altitude range is 1000–2000 m (Lu et al., 2003; Ma and Frank, 2006; Zhao et al., 2010). Oasis farming is distributed mainly over the piedmont lower alluvial fan and fluvial plain in the middle reaches of the Heihe River (Xie et al., 2012). This is the main irrigated region and an important commodity grain base in China, with a long history of agriculture and animal husbandry. About 97.3% of the total population in the Heihe River region lives in this area, producing 96.5% of the GDP of the whole basin (Fang, 2002). The lower stream is in Ejina Banner, where the annual mean precipitation is less than 50 mm and potential evapotranspiration can reach 3755 mm (Qi and Luo, 2005; Si et al., 2009). It is in the Badain Jaran Desert, with an altitude of ~1000 m (Ma and Frank, 2006). Strong winds make Ejina the main source of sandstorms in northern China (Liu et al., 2010b). Even so, the second largest *Populus euphratica* forest of China, with an area of 2.6×10^8 m^2, is in Ejina (Wang et al., 2003). It is nourished by the Heihe River, which helps form the Ejina Banner oasis. More importantly, this oasis functions as an ecological protective screen to stop desert expansion and its effect on artificial oasis.

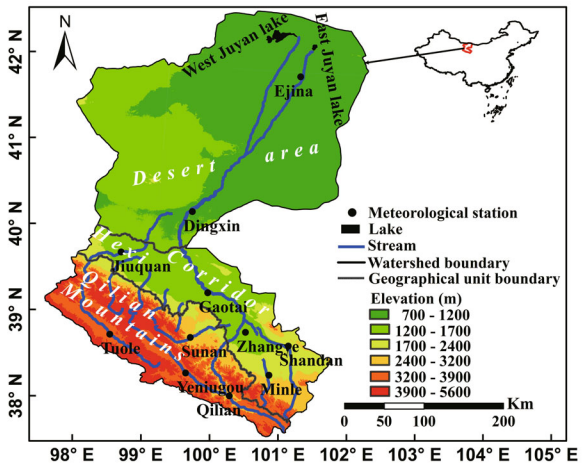

Fig. 1. Location of the study region and meteorological stations.

The Heihe basin is also an important industrial and agricultural region in western China. It includes predominantly arid and semi-arid areas, with extremely fragile ecological conditions and a low level of adaptive capacity in terms of social living conditions. There is substantial climate variability in this region and, in the future, more severe impacts on water resources, food production and ecosystem health may occur due to climate change (Zhao et al., 2005; Yin, 2006; Zhao et al., 2010; Liu et al., 2010a, 2010b; Feng et al., 2013). However, the ability of the region to adapt to a changing climate is poor, and so the development of an extreme climate will undoubtedly bring disastrous and destructive consequences.

3. Data and methods

3.1. *Data sources and processing*

Daily precipitation data from 11 rain gauge stations (Fig. 1) covering the Heihe basin were provided by the National Climate Center of the China Meteorological Administration and Gansu Meteorological Bureau. Of the 11 stations, three had missing data, but these comprised less than 0.01%. The missing data were filled in by average values of neighboring days at the same station. We believe that this gap-filling method has no significant influence on the long-term temporal trend (Zhang et al., 2011a). Data quality control was performed using the RClimDex software package (available online at http://etccdi.pacificclimate.org/software.shtml). In addition, a logarithmic transform of the monthly total precipitation amount series was carried out, before they were used as inputs for detecting homogeneity (Wang and Feng, 2010). This was accomplished with the RHtestsV3 software package (from the same website as above). The result showed that all data series used were consistent. Finally, RClimDex was used to calculate the extreme precipitation indices.

3.2. *Definition of extreme precipitation indices*

The joint Commission for Climatology (CCI)/Climate Variability and Predictability (CLIVAR)/Joint Commission for Oceanography and Marine Meteorology (JCOMM) and the Expert Team on Climate Change Detection and Indices (ETCCDI) (available online at http://www.clivar.org/organization/etccdi) developed a suite of climate change indices derived from daily precipitation and temperature data (Frich et al., 2002; Alexander et al., 2006; Klein Tank et al., 2009; Zhang et al., 2011b). The indices were based on those of the European Climate Assessment dataset and have been extensively used to study observed changes in extreme precipitation and temperature events (Klein Tank and Können, 2003; Alexander et al., 2007; Piccarreta et al., 2013; van den Besselaar et al., 2013; Fischer and Knutti, 2014). For extreme precipitation, 11 indices were defined, and software packages were developed for end-users. Considering the climate char-

acteristics of the Heihe basin, we used eight extreme precipitation indices. Because indices like the number of very heavy precipitation days (R20) and extremely wet day precipitation (R99p) are not suitable for the study area, there are many zero values in the indices, especially in the western Hexi Corridor and desert area.

3.3. *Evaluation of trends and temporal variation*

For general trends of all extreme precipitation indices at each meteorological station, the Kendall rank correlation test (Mann, 1945; Kendall, 1970; Hirsch et al., 1982) was used to detect trends in the time series. We also used the prewhitening approaches of Yue et al. (2002) to determine trends in extreme precipitation data. Meanwhile, Sen's slope method (Sen, 1968) was used to estimate trend magnitudes, based on Kendall's Tau. These were executed using the "zyp" package (Bronaugh and Werner, 2013) in the R environment (R Core Team, 2013).

The Heihe River can be divided into three sub-regions: the Qilian Mountains, Hexi Corridor, and desert area, based on their unique hydro-climate and topographical characteristics. In order to learn more about the spatial changes in those three sub-regions, regional averaged anomaly series for each index were calculated, defined as:

$$x_{r,t} = \sum_{i=1}^{n_t} (x_{i,t} - \overline{x_i})/n_t \ , \qquad (1)$$

where $x_{r,t}$ is the regionally averaged index in year t; $x_{i,t}$ is the index for station i in year t; $\overline{x_i}$ is the 1960–2011 index mean at station i; and n_t is the number of stations with data in year t. To avoid the average series being dominated by those stations with a high value, $x_{i,t}$ and $\overline{x}$ were normalized by dividing them by station standard deviation.

For the temporal variation of all extreme precipitation indices in each region during 1960–2011, fast Fourier transform (FFT) low-pass filtering and linear regression were used to smooth and calculate linear fits of annual normalized anomaly time series of extreme precipitation, respectively. Linear trends of extreme precipitation were computed using a nonparametric approach, and the trends were considered statistically significant at the 0.1 level. The related methods were executed under the origin 8.0 software.

The distribution-free cumulative sum control chart (CUSUM), cumulative deviation and Worsley likelihood ratio tests were used to test for step changes in annual normalized anomaly time series of rainfall extremes. Where significant step changes were detected, if they were found significant at the 0.1 or lower level by at least one out of three different tests, then the rank sum test and student's t-test were used to assess the significance of differences between the median and mean for time periods before and after the identified year of change. These tests were carried out using the program TREND, version 1.0.2, from the eWater Toolkit (available online at http://www.toolkit.net.au/trend). Details of the methods are described by Kundzewicz and Robson (2000) and in the TREND 1.0.2 user guide (Chiew and Siriwardena, 2005).

The three parameter generalized extreme value (GEV) distribution is based on the statistical theory of extremes (Coles, 2001). It has been widely used to simulate the behavior of precipitation extremes in both observations and models (Kharin and Zwiers, 2000; Brown et al., 2008; Wang and Zhang, 2008; Rajczak et al., 2013; Vavrus and Behnke, 2013; Jones et al., 2014). The GEV parameters (location, scale, and shape) were estimated using the method of L-moments (Hosking and Wallis, 1997); the two-sample Kolmogorov–Smirnov test (K-S test) and a parametric bootstrap were applied to detect how well the GEV fits the precipitation extreme time series and to calculate the confidence intervals for the estimated GEV parameters, respectively (Conover, 1971; Coles, 2001). All the methods were executed using the "lmomco" (Asquith, 2015) and "extRemes" (Gilleland and Katz, 2011) packages in the R environment (R Core Team, 2013).

Correlation analysis and factor analysis were used to determine which precipitation indices were selected for the analysis of changes in the PDF in each region of the basin. Factor analysis attempts to find a way to summarize the information contained in a number of original detailed variables into a smaller set of new, composite factors with a minimum loss of information (Hair et al., 2009). The resulting factors served as strategy dimensions for a cluster analysis, which was subsequently carried out on these factors (Jeswani et al., 2008). The Kaiser-Meyer-Olkin (KMO) and Bartlett's test of sphericity were used for testing for partial correlation and whether a correlation matrix was an identity matrix, respectively. The principal components method of extraction has been used in factor analysis. The procedure was implemented in the SPSS 22 software.

3.4. *Large-scale atmospheric circulation*

To quantify the relationships between large-scale atmospheric circulation and precipitation extremes, correlation analysis was used to detect the main atmospheric circulation types contributing to the extreme precipitation increase after the late 1980s. The circulation types used in this study were based on the potential factors that affected climate changes in Northwest China reported in previous studies (Zhou et al., 2009; Dong et al., 2012; Kang et al., 2012; Li et al., 2012). The selected circulation indices/types were: East Asian summer monsoon index (EASMI) (Li and Zeng, 2002, 2003), downloaded from http://ljp.lasg.ac.cn/dct/page/65540, Westerly Circulation Index (WCI) and western Pacific subtropical high intensity index (WPSHII) (for details refer to the Climate Diagnostics and Prediction Division, National Climate Center, China Meteorological Administration); and the data of Southern Oscillation Index (SOI), Multivariate ENSO Index (MEI), Pacific Decadal Oscillation (PDO), North Pacific Pattern (NP), Northern Oscillation Index (NOI), North Atlantic Oscillation (NAO) and Arctic Oscillation (AO) were taken from the National Oceanic and Atmospheric Administration (http://www.esrl.noaa.gov/psd/data/climateindices/list/).

The divergence of divergence (D) was calculated based

on the following equation (Li et al., 2009; Zhang et al., 2010; Li and Ding, 2012):

$$D = \frac{1}{g}\int_{p_s}^{p} \nabla q(u,v)dp \ , \tag{2}$$

where u and v are the zonal and meridional components of the wind field, respectively; q is specific humidity; p_s is surface pressure; and p is the pressure when the air has no water vapor. In our study, p_s was 1000 hPa and p was 300 hPa.

4. Results and analysis

4.1. *General trend of extreme precipitation*

Figure 2 reveals the spatial distribution of the general trend for extreme precipitation indices, based on Kendall's Tau and Sen's slope methods. The figure shows that non-significant trends for precipitation extremes were detected in the western Hexi Corridor and desert area; there was no consistent trend for the entire Heihe basin. For PRCPTOT, change magnitudes in the Qilian Mountains and eastern Hexi Corridor exceeded 10 mm (10 yr)$^{-1}$. Average change magnitudes of PRCPTOT were 11.38 mm (10 yr)$^{-1}$ in the Qilian Mountains and 7.57 mm (10 yr)$^{-1}$ in the Hexi Corridor. There was an increasing trend in the southern portion of the downstream part of the river [2.26 mm (10 yr)$^{-1}$] and a decreasing trend in the northern portion [-0.35 mm (10 yr)$^{-1}$]. Larger-magnitude, significant increasing trends of very wet day precipitation (R95p) were mainly in the Qilian Mountains [7.18 mm (10 yr)$^{-1}$] and eastern Hexi Corridor [5.53 mm (10 yr)$^{-1}$]. Change magnitudes for R10 in various geographic units of the Heihe basin were 0.47 d (10 yr)$^{-1}$ in the Qilian Mountains, 0.45 d (10 yr)$^{-1}$ in the eastern Hexi Corridor, and zero in the desert area. Figure 2 indicates increasing trends in the Qilian Mountains and Hexi Corridor at most stations for R$\times$1day and R$\times$5day. The SDII had an increasing trend at 9 out of the 11 stations. Large-magnitude and increasing trends in R$\times$1day, R$\times$5day and SDII were more apparent in the southern part of the lower reaches of the river than in the northern part. Figure 2 shows that CDD showed decreasing trends at all stations, except for Qilian Station in the eastern Qilian Mountains. Not including that station, which had an increase of 3.60 d (10 yr)$^{-1}$, the average change magnitude of the other three stations in the mountains was -3.89 d (10 yr)$^{-1}$; for the Hexi Corridor it was -4.10 d (10 yr)$^{-1}$, and for the desert area it was -4.41 d (10 yr)$^{-1}$. Although the CWD increasing/decreasing trends were detected based on Kendall's Tau, Sen's slope was zero at all stations.

4.2. *Temporal variation of precipitation extremes*

The temporal variation of precipitation extremes in the upper, middle and lower parts of the Heihe basin during 1960–2011 are shown in Figs. 3, 4 and 5. Figure 3 shows that statistically significant linear increasing trends were detected in six out of eight indices, all of which increased with fluctuation during 1960–2011, and PRCPTOT, R95p, SDII and R10 even had statistical significance at the 0.01 level. The significant step changes for these four indices were detected in the years 1997, 1987, and 1975/76, with the mean and median shifting before and after the change points. CWD and CDD showed no significant linear trend or step change, but it was seen from the FFT filter that they had obvious interdecadal variability. The FFT filter line in Fig. 3 displays that R$\times$1day switched from a peak to a trough and then to a peak again during 1976–1990, and the significant change point was detected in 1987. A robust step change was detected in 1970 for R$\times$5day, with statistically significant changes in the median and mean between the epochs 1960–1970 and 1971–2011.

Figure 4 reveals that, among the eight indices, only PRCPTOT, CDD and R10 had significant linear trends, and the abrupt changes were detected in the years 1986/87 and 1974 in the middle basin. For CDD, the figure shows that it had an obvious decreasing linear trend, with statistical significance at the 0.01 level and, in 87% of years, except for the early 1960s, it showed positive anomalies before 1987. After that, in 92% of years CDD had negative anomalies. CWD, R$\times$1day and R95p showed no significant linear trend or step change, but had large interannual variability (Fig. 4). The abrupt changes for R$\times$5day and SDII were detected in the years 1973 and 1969, respectively.

Figure 5 reveals that all extreme precipitation indices in the desert area showed a non-significant linear trend, but a statistically significant step change was consistently detected in 1989. All of them except CDD had obvious troughs in approximately the mid-1980s, with large interannual variability. Based on the trend extracted from the FFT filter, all indices except CDD had predominant negative anomalies at the beginning of the 1960s, and in the period of 1971–1989, especially 1980–1989.

Although temporal variations such as step changes were detected inconsistently for the different extreme precipitation indices in each geographic unit of the Heihe River, some correlations among them still existed on account of the general background of climate change over the Heihe River. The river is located near the center of the Eurasian continent and far from any ocean, which causes it to have a typically dry climate. In addition, the climate in the river basin is mainly affected by the Asian monsoon in summer and the westerlies in winter (Wang et al., 2004; Qin et al., 2010). However, rainfall in the region varies from east to west because the amounts of moisture carried by the winds are different (Xu and Gao, 2014). Precipitation in the mountainous area of the Heihe River has been revealed to possess altitude dependence in terms of its magnitude, and the maximum and minimum precipitation in this area are occurred limited to certain range of height (Tang, 1985); plus, there is also great variation in the underlying surface within each stretch of the river. Moreover, the extreme precipitation indices used in this study can reflect the amount, duration and intensity of precipitation. Therefore, although the general climate background is almost the same, extreme precipitation indices and underlying surface are obviously different, which is the reason why the temporal characteristics of precipitation extremes varied

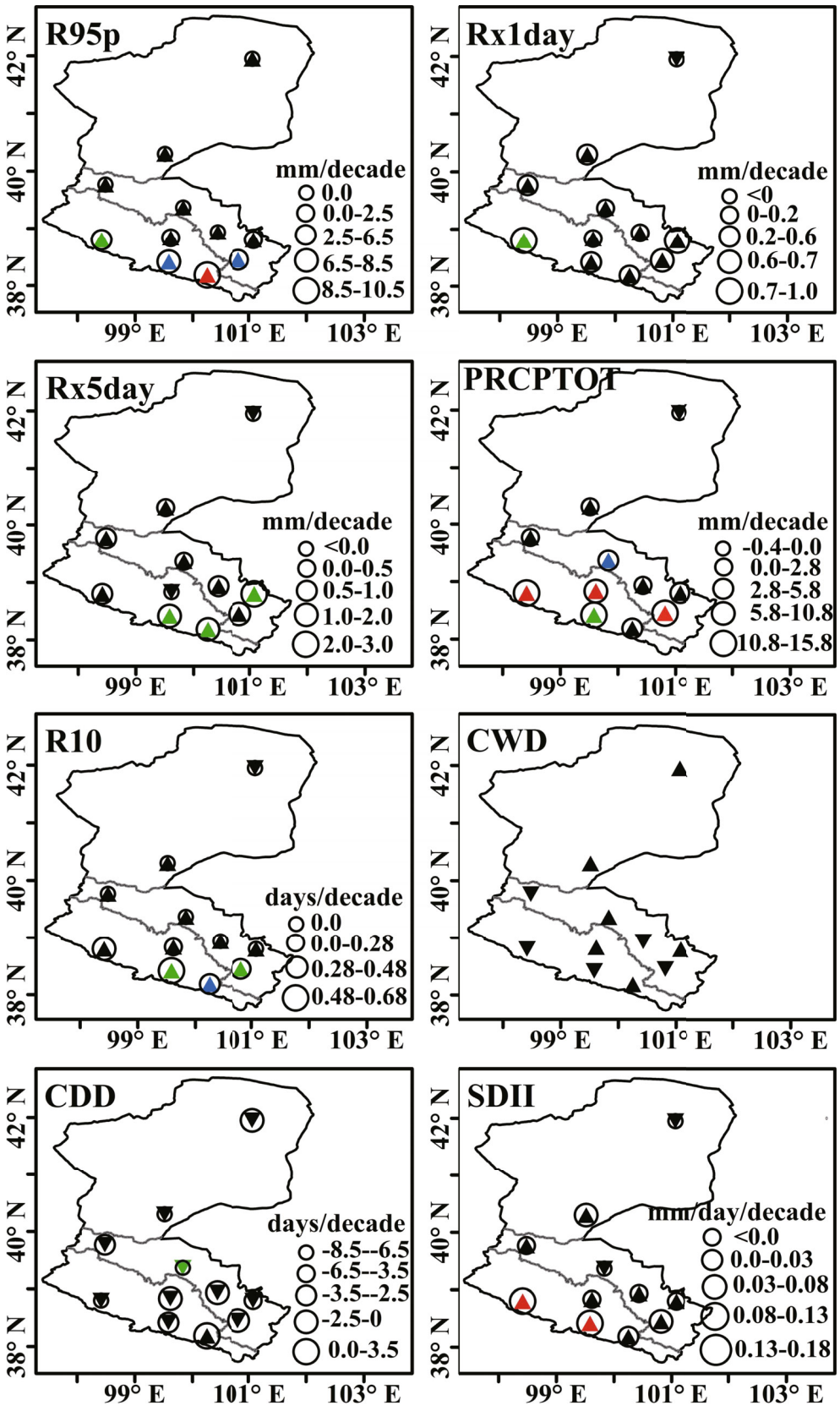

Fig. 2. Spatial distribution of the general trends in extreme precipitation indices during 1960–2011 across the Heihe River basin. Positive/negative trends are shown by up/down triangles; red, green, and blue symbols denote trends with statistical significance at the 0.01, 0.05, and 0.1 levels, respectively. The size of the black circles is proportional to the magnitude of the trend represented by Sen's slope.

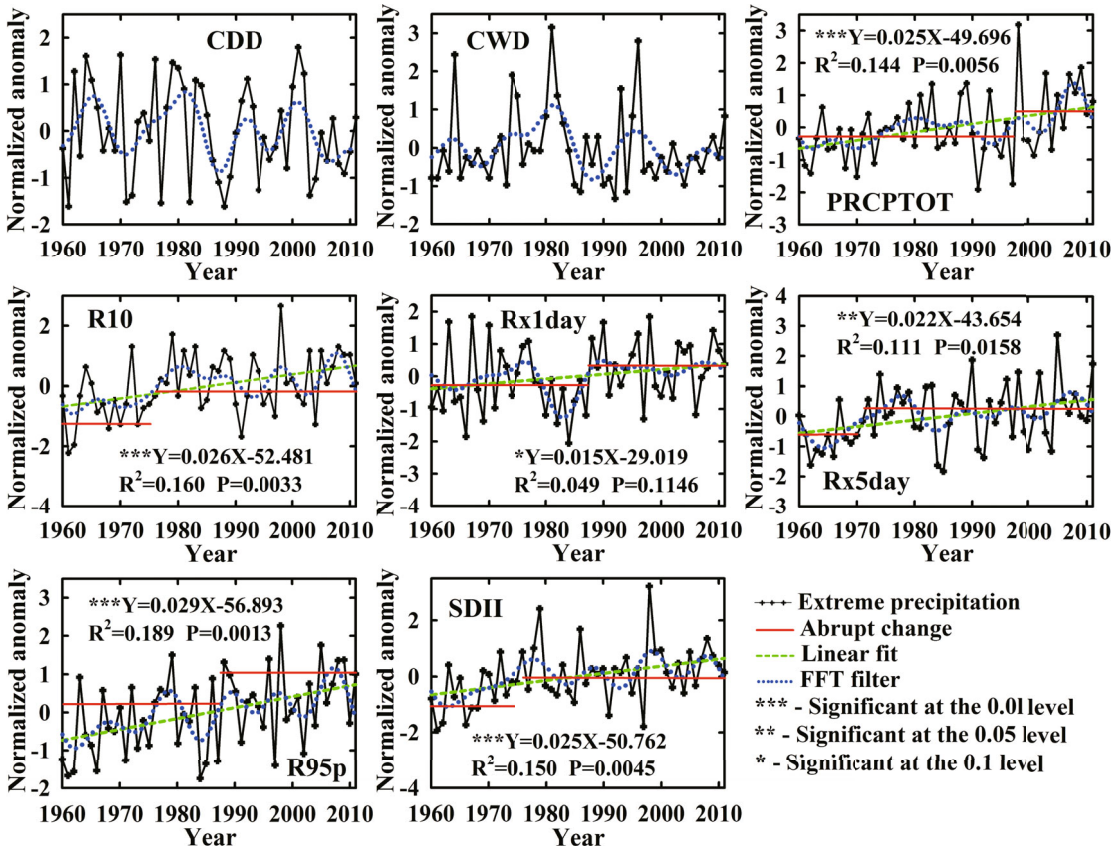

Fig. 3. Annual changes in precipitation extremes during 1960–2011 in the upstream Heihe River basin (Qilian Mountains); step changes are plotted if they were found to be significant at the 0.1 or lower level by at least one out of three different tests.

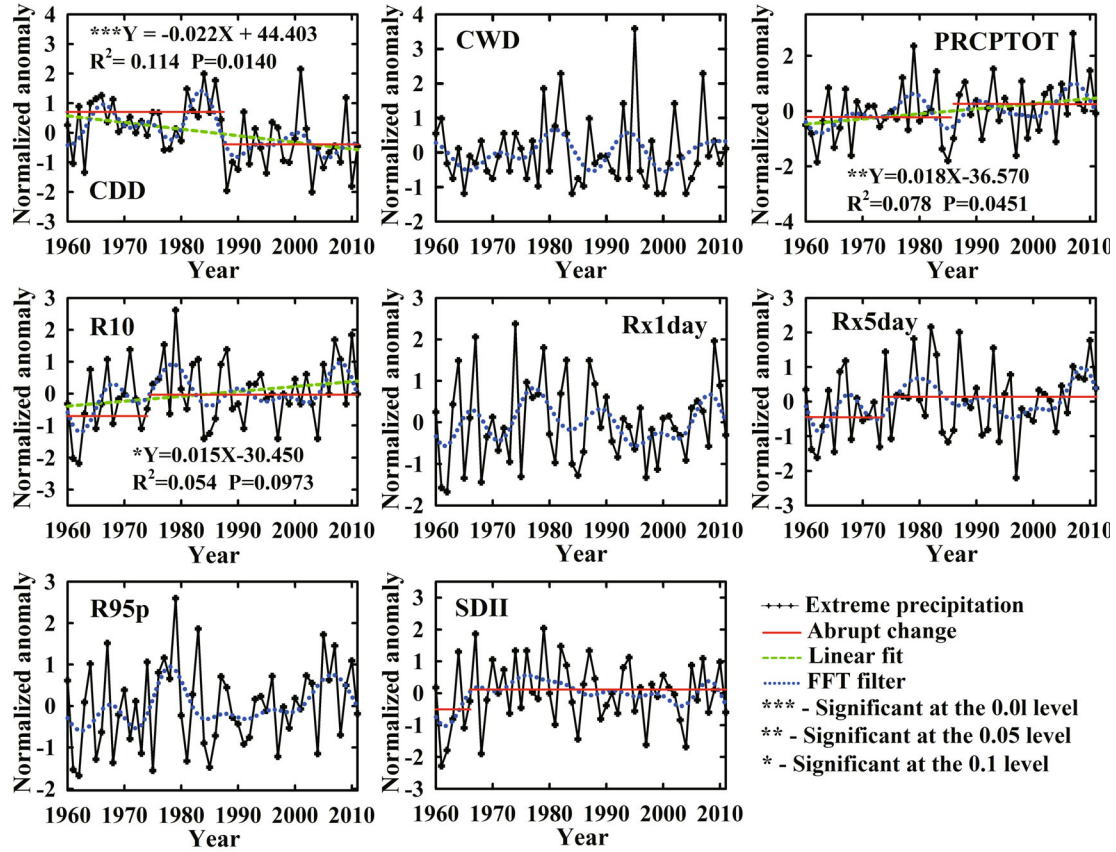

Fig. 4. As in Fig.3. but for the middle reaches of the Heihe River basin (Hexi Corridor).

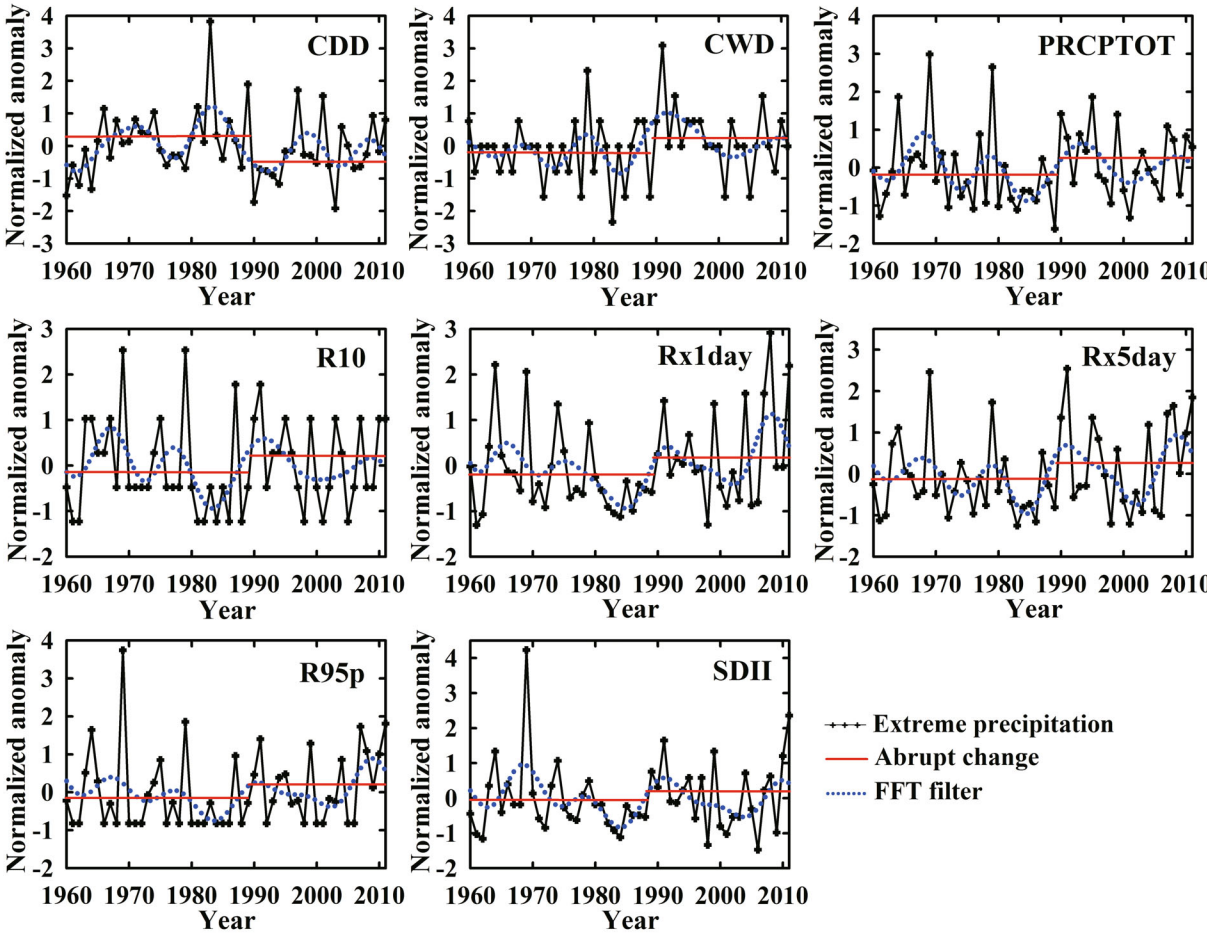

Fig. 5. As in Fig. 3. but for the downstream Heihe River basin (desert area).

in different regions.

4.3. *Probability density function*

Two types of indices were considered for analysis of the changes in the PDF: one type was indices related to extreme precipitation amount, and the other was duration of extreme precipitation. Extreme precipitation indices were selected to analyze the PDF based on correlation analysis and factor analysis (Tables 2 and 3). Pearson's correlation coefficients indicated that annual rainfall had strong correlation with most precipitation extremes indices, especially PRCPTOT and R10 in the upper and middle reaches of the Heihe River, and PRCPTOT in the downstream of the river (Table 2). Table 3 shows that loadings of the indices for the first principal component (PC1) can mainly reflect the extreme precipitation amount, and the second component (PC2) can relate to the duration of extreme precipitation. Factor analysis further confirmed that the loadings of the indices for PC1 were very high (Table 3). The significant positive factor loadings of annual rainfall were above 0.9 for PC1, indicating that the cause of annual precipitation increase is well correlated with the strength of these indices. The PC2 explained more than 13% of the data variance in each geographical unit of the Heihe River; the most statistically significant variable represented by it was CWD in the Qilian Mountains, but in the Hexi Corridor and desert area it was CDD. Therefore, PRCPTOT, R10 and CWD were selected to analyze changes in the PDF of extreme precipitation events in the Qilian Mountains, while for the Hexi Corridor PRCPTOT, R10 and CDD were chosen and, for the desert area, PRCPTOT and CDD were chosen. The results of step changes detected in Figs. 3, 4 and 5 were used to divide the period for the comparison of the PDF between two epochs, and the PDFs of extreme precipitation

Table 2. Pearson's correlation coefficients between rainfall extremes and annual rainfall in the Heihe River basin.

	Annual rainfall		
	Qilian Mountains	Hexi Corridor	Desert area
Annual rainfall	1	1	1
CDD	−0.16	−0.39*	−0.34*
CWD	0.28*	0.52*	0.60*
PRCPTOT	0.99*	0.99*	0.99*
R10	0.86*	0.84*	0.75*
R95p	0.71*	0.75*	0.76*
R×1day	0.38*	0.59*	0.64*
R×5day	0.48*	0.69*	0.76*
SDII	0.63*	0.63*	0.63*

*Significant at the 0.05 or lower level (one-tailed)

Table 3. Loadings of each variable within the first two principal components and proportional contribution to the variance in the Heihe River basin.

	Factor					
	Qilian Mountains		Hexi Corridor		Desert area	
	1	2	1	2	1	2
Annual rainfall	0.92*	0.20	0.92*	−0.29*	0.91*	−0.19
CDD	−0.17	0.36*	−0.28*	0.81*	−0.30*	0.80*
CWD	0.22	0.82*	0.51*	−0.24*	0.60*	−0.57*
PRCPTOT	0.92*	0.20	0.92*	−0.29*	0.92*	−0.19
R10	0.89*	0.17	0.88*	−0.06	0.86*	0.04
R95p	0.89*	−0.24*	0.90*	0.14	0.92*	0.24*
R×1day	0.58*	−0.55*	0.81*	0.37*	0.85*	0.28*
R×5day	0.65*	0.07	0.86*	0.18	0.93*	0.11
SDII	0.81*	−0.19	0.83*	0.42*	0.81*	0.42*
% of variance	52.83	14.65	63.32	13.84	65.93	15.03

*Pearson correlation is significant at the 0.05 or lower level (one-tailed)

are shown in Fig. 6.

Table 4 shows the goodness of fit of the GEV distribution. The table indicates that all the extreme precipitation indices in the Heihe River basin obeyed a GEV distribution, based on the K-S test. Figure 6 displays the PDF of the GEV distribution for precipitation extremes in the upper, middle and lower reaches of the river. The figure shows that, relative to the early period and 1960–2011, R10 had a pronounced increase and shift to the right during the late period in the Qilian Mountains and Hexi corridor, indicating that R10 clearly increased with time. For PRCPTOT, the PDF was positively shifted, which indicated an increase of total precipitation on wet days started in the late 1980s. Moreover, for PRCPTOT in the Qilian Mountains and desert area, the peak of extreme precipitation declined in the late period, with a flatter distribution, which confirmed the increase in PRCPTOT. The PDF of CWD displayed a higher peak in recent years as compared with the early period, and the location parameter of the GEV distribution shifted toward the left but with a long tail on the right side, indicating that very long wet spells are increasing. Average CDD showed an obvious decrease after 1987 in the Hexi Corridor, and the GEV distribution has apparently shifted toward left, with a long tail on the right side, indicating that in most years the number of CDDs decreased but,

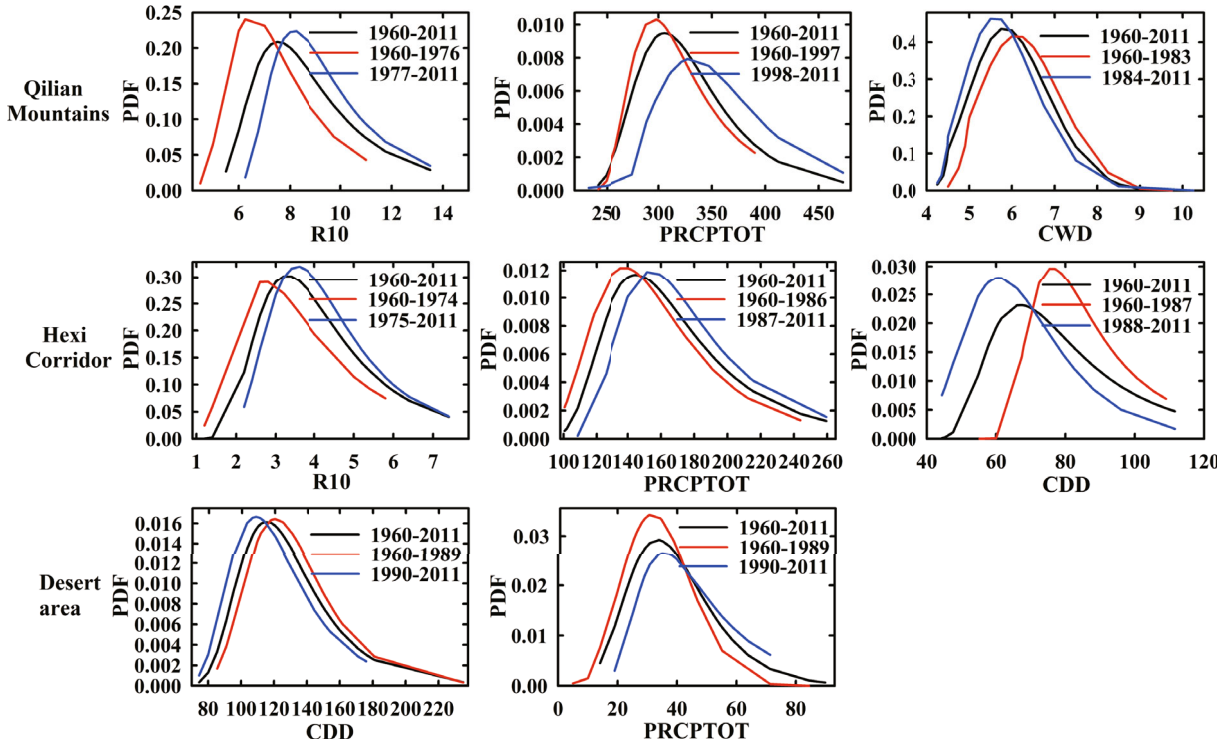

Fig. 6. PDFs of the GEV distributions for precipitation extremes in the Heihe River basin.

Table 4. The goodness-of-fit and estimated parameters of the GEV distribution.

Region	Index	Estimated parameters (95% confidence interval)			K-S test		
		Location	Scale	Shape	*D*	*P*	Dis
Qilian Mountains	R10	7.92 [7.36, 8.42]	1.81 [1.42, 2.20]	−0.25 [−0.45, −0.05]	0.10	0.69	GEV
	R10_1	6.82 [5.98, 7.65]	1.54 [0.94, 2.08]	−0.24 [−0.63, 0.11]	0.17	0.63	GEV
	R10_2	8.58 [7.98, 9.17]	1.71 [1.25, 2.12]	−0.29 [−0.56, −0.05]	0.09	0.91	GEV
	PRCPTOT	308.58 [297.16, 320.65]	38.92 [30.84, 48.59]	−0.08 [−0.30, 0.09]	0.11	0.56	GEV
	PRCPTOT_1	303.14 [291.09, 315.54]	36.49 [26.27, 45.22]	−0.23 [−0.48, 0]	0.12	0.63	GEV
	PRCPTOT_2	333.31 [307.55, 364.70]	46.32 [24.98, 69.72]	−0.05 [−0.53, 0.32]	0.11	0.99	GEV
	CWD	5.66 [5.43, 5.99]	0.85 [0.64, 1.10]	0.19 [−0.05, 0.42]	0.08	0.85	GEV
	CWD_1	5.88 [5.54, 6.38]	0.90 [0.56, 1.36]	0.23 [−0.16, 0.54]	0.11	0.87	GEV
	CWD_2	5.49 [5.17, 5.85]	0.80 [0.52, 1.12]	0.15 [−0.17, 0.46]	0.09	0.95	GEV
Hexi Corridor	R10	3.52 [3.16, 3.89]	1.24 [0.99, 1.50]	−0.21 [−0.43, −0.01]	0.08	0.83	GEV
	R10_1	3.01 [2.32, 3.78]	1.30 [0.78, 1.88]	−0.27 [−0.72, 0.12]	0.15	0.86	GEV
	R10_2	3.73 [3.33, 4.18]	1.16 [0.89, 1.47]	−0.17 [−0.42, 0.03]	0.08	0.94	GEV
	PRCPTOT	150.12 [141.05, 160.21]	32.05 [24.52, 39.03]	−0.18 [−0.39, 0]	0.06	0.97	GEV
	PRCPTOT_1	141.33 [128.89, 152.74]	30.41 [21.71, 40.76]	−0.13 [−0.44, 0.12]	0.10	0.94	GEV
	PRCPTOT_2	159.83 [145.17, 174.27]	31.58 [21.79, 41.37]	−0.22 [−0.57, 0.06]	0.12	0.83	GEV
	CDD	71.19 [66.16, 76.49]	16.55 [13.24, 20.23]	−0.30 [−0.53, −0.10]	0.07	0.95	GEV
	CDD_1	80.20 [75.23, 86.04]	13.22 [9.69, 16.61]	−0.38 [−0.70, −0.11]	0.09	0.98	GEV
	CDD_2	61.11 [55.66, 67.86]	13.16 [8.51, 17.75]	−0.02 [−0.38, 0.26]	0.08	0.99	GEV
Desert area	PRCPTOT	32.91 [29.24, 36.95]	12.59 [9.77, 16.14]	0.04 [−0.18, 0.25]	0.06	0.99	GEV
	PRCPTOT_1	29.51 [25.43, 34.71]	10.88 [7.52, 15.11]	0.19 [−0.18, 0.46]	0.09	0.96	GEV
	PRCPTOT_2	38.52 [31.62, 45.20]	14.20 [9.69, 19.20]	−0.23 [−0.61, 0.09]	0.10	0.94	GEV
	CDD	116.19 [108.99, 123.79]	22.80 [17.92, 28.27]	−0.06 [−0.28, 0.13]	0.09	0.80	GEV
	CDD_1	120.58 [111.72, 129.47]	22.39 [15.52, 29.93]	−0.02 [−0.35, 0.22]	0.09	0.93	GEV
	CDD_2	110.29 [101.29, 121.63]	22.20 [14.60, 30.26]	−0.09 [−0.43, 0.19]	0.14	0.74	GEV

D is the K-S test statistic, and *P* and *D* are abbreviations for probability and distribution, respectively. R10 covers the period from 1960 to 2011, and R10_1 and R10_2 use the early and late period, respectively, divided by the year of step change. The same denotation is used for the other indices. The units of location and scale parameters are the same as the corresponding indices.

meanwhile, much longer consecutive dry days occurred in recent years. The PDF of CDD in 1960–1989 in the desert area showed a shift toward the right and had a long right tail, indicating that the number of CDDs during 1990–2011 decreased with time.

4.4. *Atmospheric circulation underlying the changes in precipitation extremes*

The Heihe River is located at the intersection of monsoonal and westerly circulation (Qin et al., 2010). High monthly rainfall amounts over the river are mainly concentrated from May to September, and the heaviest rain occurs in July, implying that the Asian monsoon plays an important role in changes in precipitation over the river. In addition, water vapor in the atmosphere can be affected by westerly winds in the region (Wang et al., 2004), and the influence of these winds are strengthened as the winter monsoon prevails in the region. The western and eastern parts of the upper Heihe River are located on the mountain slopes of the westerlies and southeast monsoon, respectively. Therefore, these can cause more rainfall and extremes have been occurring in the mountainous area of the river. However, rainfall in the region varies from east to west because the amounts of moisture carried by the winds are different (Xu and Gao, 2014). The western Pacific subtropical high, which occupies about 20%–25% of the Northern Hemisphere's surface, plays a major role in the global circulation of the atmosphere and oceans (Liu and Wu, 2004). It has been identified as an important component of the East Asian summer monsoon system and has predominance in the East Asian climate (Lau and Li, 1984; Huang and Wu, 1989).

The effects of large-scale circulation types, as discussed above, are confirmed by the Pearson's correlation coefficients presented in Table 5. The table shows that precipitation extremes in the Qilian Mountains and Hexi Corridor had strong and significant correlation with EASMI and WPSHII. For all the other tested atmospheric circulation types, the correlations were much weaker and less significant. Another feature worth mentioning is that nearly all the correlations in the desert area were non-significant, which indicates that the impacts of large-scale atmospheric circulation types on changes in extreme precipitation are less in the area. The apparently negative correlation between the EASMI and rainfall extremes indicates that a weak East Asian summer monsoon can result in changes in the amount, frequency and intensity of rainfall in the upper and middle reaches of the Heihe River. Yu et al. (2004) indicated that the East Asian summer monsoon has experienced significant weakening. Ding et al. (2008, 2009) confirmed that an anomalously strong summer monsoon flow in 1951–1978 shifted to an anomalously weak monsoon flow after 1978; the significant weakening of the component of the tropical upper-level easterly jet has made a

Table 5. Pearson's correlation coefficients between rainfall extremes in the Heihe River basin and large-scale atmospheric circulation indices/types.

Region	Index	EASMI	WCI	WPSHII	SOI	MEI	PDO	NP	NOI	NAO	AO
Qilian Mountains	R10	−0.41*	0.02	0.41*	−0.07	0.25*	0.27*	−0.11	−0.34*	0.04	0.03
	PRCPTOT	−0.44*	−0.02	0.36*	0.11	0.04	0.13	−0.02	−0.14	0.03	0.12
	CWD	−0.19	−0.30*	−0.07	0.19	−0.14	0.11	−0.01	−0.01	−0.08	−0.08
Hexi Corridor	R10	−0.47*	−0.02	0.27*	0.05	0.03	0.06	−0.01	−0.18	−0.03	0.04
	PRCPTOT	−0.49*	0.03	0.47*	−0.03	0.13	0.16	−0.11	−0.31*	0.04	0.09
	CDD	0.27*	−0.22	−0.45*	−0.07	0.01	0.01	0.00	0.07	−0.02	−0.18
Desert area	PRCPTOT	−0.19	0.06	0.19	0.03	−0.04	−0.09	0.04	−0.11	−0.07	−0.07
	CDD	−0.13	−0.21	−0.09	−0.03	0.12	0.16	−0.27*	−0.23	0.00	−0.08

*Significant at the 0.05 or lower level (one-tailed)

dominant contribution to the weakening of the Asian summer monsoon system.

Table 5 indicates that WPSHII had significantly positive correlations with R10 and PRCPTOT, which means that changes in WPSHII will have large impacts on rainfall extremes in the upper and middle reaches of the Heihe River. The Kendall rank correlation test indicated that an apparent linear increasing trend with statistical significance at the 0.01 level was detected in WPSHII; the step changes tests consistently showed statistically significant WPSHII change in 1986, with median and mean values for the 1960–1986 and 1987–2011 periods being significantly different (Fig. 7). Therefore, the increase in WPSHII could be interpreted as more extreme rainfall in the late 1980s.

Climate variability and change in Northwest China, from warm and dry to warm and wet, occurred after the 1970s, with an abrupt change in 1987 (Yin, 2006; Shi et al., 2007). In addition, Liu et al. (2010b) found a significant cycle of annual precipitation around 1980 (1978–1982) in the Heihe River region, based on tree-ring width analysis. Step changes in precipitation extremes examined in this study mainly occurred in the late 1980s (Table 4). IPCC (2013) indicated that a weakened monsoon will result in a monsoonal rainfall decrease, but this can be compensated for by increased atmospheric moisture content, leading to more precipitation and extremes. To investigate the changes in water vapor flux after the late 1980s, as compared with the earlier period, composite circulation maps from the National Centers for Environmental Prediction/National Center for Atmospheric Research reanalysis data for the wet season (May–September) were created for the two epochs (1960–1987 and 1988–2011) and their difference (the former subtracted from the latter). The selected region was (10°–70°N, 40°–160°E). Figure 8 shows an obvious negative value of water vapor flux divergence occurred over the entire Heihe River, implying that there were large amounts of water vapor in the wet season during 1988–2011. This can explain the increase in extreme precipitation over the basin after the late 1980s.

Local climate conditions are predominantly controlled by large-scale forcing in Northwest China, and land surface forcing also has a significant impact (Wen and Jin, 2012). Land surface processes determine the water, energy and momentum flux to the atmosphere (IPCC, 2001). Therefore, land

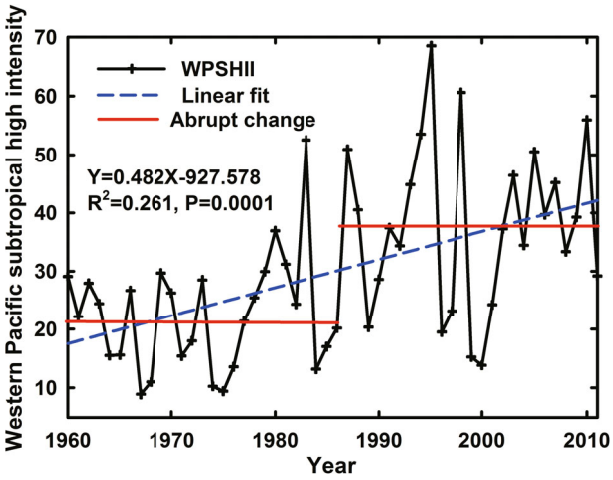

Fig. 7. Temporal variation in western Pacific subtropical high intensity index (WPSHII) from 1960 to 2011.

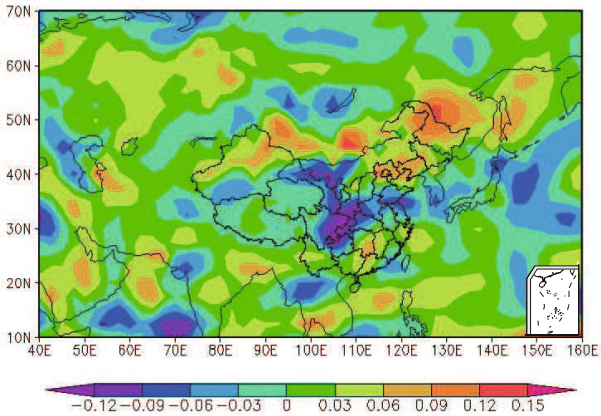

Fig. 8. Difference in water vapor flux divergence (g m^{-2} s^{-1}) between 1960–1987 and 1988–2011 in the wet season.

surface–atmosphere interaction is essential to the climate and also plays a crucial role in increases in climate variability (Seneviratne et al., 2006). The partitioning of precipitation into evapotranspiration is highly dependent on the moisture status of the land surface, especially the amount of soil moisture available for evapotranspiration, which in turn depends

on properties of the land cover (IPCC, 2013). Convective precipitation can be enhanced by mesoscale variation in vegetation cover, especially in semi-arid areas (Anthes, 1984). Enhanced land surface characteristics have a stronger impact on atmospheric water vapor fields in the lower boundary layer than other meteorological fields in the Heihe River basin (Gao et al., 2008). Barren land has greatly decreased in the upper and lower reaches of the Heihe River from 1987 to 2002, while cropland and urban or built-up land have increased largely in the midstream of the river (Qi and Luo, 2005). Wang et al. (2007) investigated land use in four years (1950, 1967, 1986, and 2000) in the middle reaches of Heihe river and found that the natural grassland area has diminished significantly and been replaced mostly by cultivated and desertified lands since 1967. The Land-Use and Cover-Change (LUCC) shows an obvious change from 1990–2000 to 2000–2006 in the lower reaches of the Heihe River due to the implementation of a water resources redistribution policy (Wang et al., 2011). The spatiotemporal variance of the impacts of LUCC on the energy and water balance of the Heihe River indicates that different land use/cover conversions can result in various energy balances, and the most significant impact on the surface energy balance occurs when grassland is converted to barren land or sparsely vegetated land (Deng et al., 2015). Therefore, changes in land surface characteristics in the Heihe River basin in recent years are one of the reasons for changes in extreme precipitation events in this region.

5. Conclusion and discussion

A typical arid region was selected to study the trends and temporal variation in rainfall extremes, based on daily precipitation datasets at 11 stations across the Heihe River basin of Northwest China from 1960 to 2011. Their changes caused by large-scale atmospheric circulation were also analyzed. The general trend of extreme precipitation events in the basin showed apparent spatial patterns. All the indices representing rainfall amount showed a basin-wide increase, except the northern desert area. The most noteworthy feature was the prevalent downward trend of CDD at nearly all stations in the basin. CWD was the most diversified index in the region. For the upstream area and eastern part of the middle basin, PRCPTOT, R95p, R×5day, and R10 had increasing trends, and most were of large magnitude. In the lower basin the trends in precipitation indices varied strongly from south to north, and more extreme precipitation events occurred in southern parts of the desert area.

Statistically significant linear trends and step changes were detected for all extreme precipitation indices, except CDD and CWD, in the Qilian Mountains, and the mean and median were also significantly shifted before and after the change points. For the middle part of the basin, it had a robust decreasing linear trend in CDD and a step change was detected in 1987. All the extreme rainfall indices showed large interannual variability in the desert area and step changes in 1989. Large-scale atmospheric circulation indices, such as EASMI and WPSHII, changes in land surface processes, and increased water vapor contributed to the change in precipitation extremes in the Heihe River region.

Climate extremes are defined as the occurrence of a value of a climate variable above (or below) a threshold value near the upper (or lower) ends of the range of observed values of the variable (IPCC, 2012). A specified base period is often used to determine the threshold value. Of particular importance is that inhomogeneity exists at the boundaries of the climatological base period used to compute the thresholds for percentiles (Alexander et al., 2006). Therefore, different base periods can result in changes in climate extremes, especially in their absolute values. The selection of an appropriate threshold is a crucial step for the application of the peak over threshold approach with a Generalized Pareto Distribution (GPD) (Saidi et al., 2013). The GPD fit is highly sensitive to threshold selection (Sanabria and Cechet, 2010). Therefore, the base period used to calculate the threshold can have a great effect on methods more sensitive to thresholds in the modeling of extreme climate events. Among the eight extreme climate indices used in our study, only R95p was dependent on the base period. However, we only analyzed the temporal variation and trend for R95p, and those features were less affected by the threshold value. Therefore, more attention should be given to the threshold value obtained from different base periods in future research, when applying methods sensitive to threshold values in climate extreme analyses.

The step changes for most extreme precipitation indices in the Heihe River basin that occurred in about the late 1980s show consistency with that reported in Northwest China (Chen et al., 2014). Precipitation extremes possess obvious regional variation both in the Heihe River basin and in Northwest China (Deng et al., 2014). High intensity, statistical significance, and large-magnitude trends for all the extreme precipitation indices were detected in the Qilian Mountains and eastern Hexi Corridor. Moreover, although most precipitation extremes have shown increasing trends both in the Heihe River basin and Northwest China, a larger magnitude for PRCPTOT was found in our study area, especially in the Qilian Mountains (Wang et al., 2012). This is because mountainous areas and climatic intersection zones are more sensitive to climate change (Loarie et al., 2009; Qin et al., 2010; Liu et al., 2010b). The EASMI and WPSHII showed significant correlation with rainfall extremes in the upper and middle reaches of the river, but their temporal variation was different in the two regions. These findings suggest that future research might need to focus more on land surface–atmosphere interactions at the local scale.

This study contributes positively to our understanding of the spatiotemporal variation in extreme precipitation in the Heihe River basin under climate change, strengthening water resources management at the basin scale and preventing and mitigating impacts on the regional environment. Thus, our study helps lay the foundations for assessing the impact of climate change on water resources in arid inland river basins and their levels of ecological adaptability.

Acknowledgements. This work was supported by the Key Project of the Chinese Academy of Sciences (Grant No. KZZD-EW-04-05). Guobin FU was supported by the Australia–China Joint Research Centre on River Basin Management. We are grateful for the free R software (version 3.1.1), which enabled convenient and time-saving calculations.

REFERENCES

Aguilar, E., and Coauthors, 2005: Changes in precipitation and temperature extremes in Central America and northern South America, 1961–2003. *J. Geophys. Res.*, **110**, D23107, doi: 10.1029/2005JD006119.

Alexander, L. V., P. Hope, D. Collins, B. Trewin, A. Lynch, and N. Nicholls, 2007: Trends in Australia's climate means and extremes: a global context. *Aust. Meteor. Mag.*, **56**, 1–18.

Alexander, and Coauthors, 2006: Global observed changes in daily climate extremes of temperature and precipitation. *J. Geophys. Res.*, **111**, D05109, doi: 10.1029/2005JD006290.

Anthes, R. A., 1984: Enhancement of convective precipitation by mesoscale variations in vegetative covering in semiarid regions. *J. Climate Appl. Meteor.*, **23**, 541–554, doi: 10.1175/1520-0450(1984)023<0541:EOCPBM>2.0.CO;2

Asquith, W., 2015: *L-moments*, *Censored L-moments*, *Trimmed L-moments*, *L-comoments*, *and Many Distributions*. R package version 2.1.4, 532 pp. [Available online at http://www.cran.r-project.org/package=lmomco.]

Bronaugh, D., and A. Werner, 2013: *zyp: Zhang + Yue-Pilon trends package*. R package version 0. 10-1, 9 pp. [Available online at http://CRAN.R-project.org/package=zyp.]

Brown, S. J., J. Caesar, and C. A. T. Ferro, 2008: Global changes in extreme daily temperature since 1950. *J. Geophys. Res.*, **113**, D05115, doi: 10.1029/2006JD008091.

Chen, Y. N., H. J. Deng, B. F. Li, Z. Li, and C. C. Xu, 2014: Abrupt change of temperature and precipitation extremes in the arid region of Northwest China. *Quaternary International*, **336**, 35–43, doi: 10.1016/j.quaint.2013.12.057.

Cheng, G. D., X. Li, W. Z. Zhao, Z. M. Xu, Q. Feng, S. C. Xiao, and H. L. Xiao, 2014: Integrated study of the water-ecosystem-economy in the Heihe River Basin. *National Science Review*, **1**, 413–428, doi: 10.1093/nsr/nwu017.

Chiang, S.-H., and K.-T. Chang, 2011: The potential impact of climate change on typhoon-triggered landslides in Taiwan, 2010–2099. *Geomorphology*, **133**, 143–151, doi: 10.1016/j.geomorph.2010.12.028.

Chiew, F., and L. Siriwardena, 2005: TREND user guide, 23 pp. [Available online at http://www.toolkit.net.au/Tools/DownloadDocumentation.aspx?id=1000134.]

Choi, G., and Coauthors, 2009: Changes in means and extreme events of temperature and precipitation in the Asia-Pacific Network region, 1955–2007. *Int. J. Climatol.*, **29**, 1906–1925, doi: 10.1002/joc.1979.

Coles, S., 2001: *An Introduction to Statistical Modeling of Extreme Values*. Springer-Verlag, London, 208 pp.

Conover, W. J., 1971: *Practical Nonparametric Statistics*. Wiley, New York, 462 pp.

Deng, H. J., Y. N. Chen, X. Shi, W. H. Li, H. J. Wang, S. H. Zhang, and G. H. Fang, 2014: Dynamics of temperature and precipitation extremes and their spatial variation in the arid region of northwest China. *Atmospheric Research*, **138**, 346–355, doi: 10.1016/j.atmosres.2013.12.001.

Deng, X. Z., Q. L. Shi, Q. Zhang, C. C. Shi, and F. Yin, 2015: Impacts of land use and land cover changes on surface energy and water balance in the Heihe River Basin of China, 2000–2010. *Physics and Chemistry of the Earth*, *Parts A/B/C*, doi: 10.1016/j.pce.2015.01.002.

Ding, Y. H. , Y. Sun, Z. Y. Wang, Y. X. Zhu, and Y. F. Song, 2009: Inter-decadal variation of the summer precipitation in China and its association with decreasing Asian summer monsoon Part II: Possible causes. *Int. J. Climatol.*, **29**, 1926–1944, doi: 10.1002/joc.1759.

Ding, Y. H., Z. Y. Wang, and Y. Sun, 2008: Inter-decadal variation of the summer precipitation in East China and its association with decreasing Asian summer monsoon. Part I: Observed evidences. *Int. J. Climatol.*, **28**, 1139–1161, doi: 10.1002/joc.1615.

Donat, M. G., and Coauthors, 2013: Updated analyses of temperature and precipitation extreme indices since the beginning of the twentieth century: The HadEX2 dataset. *J. Geophys. Res.*, **118**, 2098–2118, doi: 10.1002/jgrd.50150.

Dong, D.-Y., S.-W. Wang, and J.-H. Zhu, 2012: East Asian winter monsoon and Arctic Oscillation. *Geophys. Res. Lett.*, **28**, 2073–2076, doi: 10.1029/2000GL012311.

Fang, C.-L., 2002: Discrepancy laws of the eco-economic zone in Heihe drainage area and its coupling development pattern. *Acta Ecologica Sinica*, **22**, 659–668. (in Chinese with English abstract)

Feng, J., D. Yan, C. Li, Y. Gao., and J. Liu, 2014: Regional frequency analysis of extreme precipitation after drought events in the Heihe River basin, Northwest China. *Journal of Hydrologic Engineering*, **19**, 1101–1112, doi: 10.1061/(ASCE)HE.1943-5584.0000903.

Feng, Q., W. Liu, and H. Y. Xi, 2013: Comprehensive evaluation and indicator system of land desertification in the Heihe River basin. *Nature Hazards*, **65**, 1573–1588, doi: 10.1007/s11069-012-0429-5.

Fischer, E. M., and R. Knutti, 2014: Detection of spatially aggregated changes in temperature and precipitation extremes. *Geophys. Res. Lett.*, **41**, 547–554, doi: 10.1002/2013GL058499.

Frich, P., L. V. Alexander, P. Della-Marta, B. Gleason, M. Haylock, A. M. G. Klein Tank, and T. Peterson, 2002: Observed coherent changes in climatic extremes during the second half of the twentieth century. *Climate Research*, **19**, 193–212, doi: 10.3354/cr019193.

Fu, G. B., J. J. Yu, X. B. Yu, R. Ouyang, Y. C. Zhang, P. Wang, W. B. Liu, and L. L. Min, 2013: Temporal variation of extreme rainfall events in China, 1961–2009. *J. Hydrol.*, **487**, 48–59, doi: 10.1016/j.jhydrol.2013.02.021.

Fu, G. B., N. R. Viney, S. P. Charles, and J. R. Liu, 2010: Long-term temporal variation of extreme rainfall events in Australia: 1910–2006. *Journal of Hydrometeorology*, **11**, 950–965, doi: 10.1175/2010JHM1204.1.

Gao, Y. H., and Coauthors, 2008: Enhancement of land surface information and its impact on atmospheric modeling in the Heihe River Basin, northwest China. *J. Geophys. Res.*, **113**, D20S90, doi: 10.1029/2008JD010359.

Gilleland, E., and R.W. Katz, 2011: New software to analyze how extremes change over time. *Eos*, **92**, 13–14, doi: 10.1029/2011EO020001.

Grant, O. M., L. Tronina, J. C. Ramalho, C. Kurz Besson, R. Lobo-do-Vale, J. Santos Pereira, H. G. Jones, and M. M. Chaves, 2010: The impact of drought on leaf physiology of *Quercus suber* L. trees: Comparison of an extreme drought event with

chronic rainfall reduction. *Journal of Experimental Botany*, **61**, 4361–4371, doi: 10.1093/jxb/erq239.

Gregersen, I. B., H. J. D. Sørup, H. Madsen, D. Rosbjerg, P. S. Mikkelsen, and K. Arnbjerg-Nielsen, 2013: Assessing future climatic changes of rainfall extremes at small spatio-temporal scales. *Climatic Change*, **118**, 783–797, doi: 10.1007/s10584-012-0669-0.

Groisman, P. Y., R. W. Knight, D. R. Easterling, T. R. Karl, G. C. Hegerl, and V. N. Razuvaev, 2005: Trends in intense precipitation in the climate record. *J. Climate*, **18**, 1326–1350, doi: 10.1175/JCLI3339.1.

Hair, J. F., W. C. Black, B. J. Babin, and R. E. Anderson, 2009: *Multivariate Data Analysis*. 7th ed. Prentice Hall, New Jersey, 816 pp.

Heisler-white, J., J. M. Blair, E. F. Kelly, K. Harmoney, and A. K. Knapp, 2009: Contingent productivity responses to more extreme rainfall regimes across a grassland biome. *Global Change Biology*, **15**, 2894–2904, doi: 10.1111/j.1365-2486.2009.01961.x.

Hirsch, R. M., J. R. Slack, and R. A. Smith, 1982: Techniques of trend analysis for monthly water quality data. *Water Resour. Res.*, **18**, 107–121, doi: 10.1029/WR018i001p00107.

Hosking, J. R. M., and J. R. Wallis, 1997: *Regional Frequency Analysis: An Approach Based on L-Moments*. Cambridge University Press, 242 pp.

Hossain, F., I. Jeyachandran, and R. Pielke Jr., 2010: Dam safety effects due to human alteration of extreme precipitation. *Water Resour. Res.*, **46**, W03301, doi: 10.1029/2009WR007704.

Huang, R. H., and Y. F. Wu, 1989: The influence of ENSO on the summer climate change in China and its mechanism. *Adv. Atmos. Sci.*, **6**, 21–32, doi: 10.1007/BF02656915.

IPCC, 2001: Climate change 2001: The scientific basis. *Contribution of Working Group I to the Third Assessment Report of the Intergovernmental Panel on Climate Change*. Houghton et al., Eds., Cambridge University Press, Cambridge, 881 pp.

IPCC, 2012: Managing the risks of extreme events and disasters to advance climate change adaptation. *A special report of Working Groups I and II of the Intergovernmental Panel on Climate Change*. Field et al., Eds., Cambridge University Press, Cambridge, 582 pp.

IPCC, 2013: Climate change 2013: the physical science basis. *Contribution of Working Group I to the Fifth Assessment Report of the Intergovernmental Panel on Climate Change*. Stocker et al., Eds., Cambridge University Press, Cambridge, 1535 pp.

Jeswani, H. K., W. Wehrmeyer, and Y. Mulugetta, 2008: How warm is the corporate response to climate change? Evidence from Pakistan and the UK. *Business Strategy and the Environment*, **18**, 46–60, doi: 10.1002/bse.569.

Jones, M. R., S. Blenkinsop, H. J. Fowler, and C. G. Kilsby, 2014: Objective classification of extreme rainfall regions for the UK and updated estimates of trends in regional extreme rainfall. *Int. J. Climatol.*, **34**, 751–765, doi: 10.1002/joc.3720.

Kang, E., G. D. Cheng, K. C. Song, B. Jin, X. D. Liu, and J. Y. Wang, 2005: Simulation of energy and water balance in Soil-Vegetation- Atmosphere Transfer system in the mountain area of Heihe River Basin at Hexi Corridor of Northwest China. *Science in China* (*D*), **48**, 538–548, doi: 10.1360/02yd0428.

Kang, S. Y., B. Yang, and C. Qin, 2012: Recent tree-growth reduction in north central China as a combined result of a weakened monsoon and atmospheric oscillations. *Climatic Change*, **115**, 519–536, doi: 10.1007/s10584-012-0440-6.

Kendall, M. G., 1970: *Rank Correlation Methods*. Griffin, London, 202 pp.

Kharin, V. V., and F. W. Zwiers, 2000: Changes in the extremes in an ensemble of transient climate simulations with a coupled atmosphere-ocean GCM. *J. Climate*, **13**, 3760–3788, doi: 10.1175/1520-0442(2000)013<3760:CITEIA>2.0.CO;2.

Kiktev, D., J. Caesar, L. V. Alexander, H. Shiogama, and M. Collier, 2007: Comparison of observed and multi-modeled trends in annual extremes of temperature and precipitation. *Geophys. Res. Lett.*, **34**, L10702, doi: 10.1029/2007GL029539.

Klein Tank, A. M. G., and G. P. Können, 2003: Trends in indices of daily temperature and precipitation extremes in Europe, 1946–99. *J. Climate*, **16**, 3665–3680, doi: 10.1175/1520-0442(2003)016<3665:TIIODT>2.0.CO;2.

Klein Tank, A. M. G., F. W. Zwiers, and X. Zhang, 2009: Guidelines on analysis of extremes in a changing climate in support of informed decisions for adaptation. Climate Data and Monitoring, WCDMP-No. 72, WMO-TD No. 1500, 56 pp.

Klein Tank, A. M. G., and Coauthors, 2006: Changes in daily temperature and precipitation extremes in central and south Asia. *J. Geophys. Res.*, **111**, D16105, doi: 10.1029/2005JD006316.

Knapp, A. K., and Coauthors, 2008: Consequences of more extreme precipitation regimes for terrestrial ecosystems. *Bioscience*, **58**, 811–821, doi: 10.1641/B580908.

Kundzewicz, Z. W., and A. Robson, 2000: Detecting Trend and Other Changes in Hydrological Data. World Climate Program-Water, WMO/UNESCO, WCDMP-45, WMO/TD 1013, Geneva, 157 pp.

Kunkel, K. E., D. R. Easterling, D. A. R. Kristovich, B. Gleason, L. Stoecker, and R. Smith, 2012: Meteorological causes of the secular variations in observed extreme precipitation events for the conterminous United States. *Journal of Hydrometeorology*, **13**, 1131–1141, doi: 10.1175/JHM-D-11-0108.1.

Lau, K.-M., and M.-T. Li, 1984: The monsoon of East Asia and its global associations—A survey. *Bull. Amer. Meteor. Soc.*, **65**, 114–125, doi: 10.1175/1520-0477(1984)065<0114:TMOEAA>2.0.CO;2.

Li, B. F., Y. N. Chen, and X. Shi, 2012: Why does the temperature rise faster in the arid region of Northwest China? *J. Geophys. Res.*, **117**, D16115, doi: 10.1029/2012JD017953.

Li, H.-Y., Z.-H. Lin, and H. Chen, 2009: Interdecadal variability of spring precipitation over South China and its associated atmospheric water vapor transport. *Atmos. Oceanic Sci. Lett.*, **2**, 113–118.

Li, J. P., and Q. C. Zeng, 2002: A unified monsoon index. *Geophys. Res. Lett.*, **29**, 1151–1154, doi: 10.1029/2001GL013874.

Li, J. P., and Q. C. Zeng, 2003: A new monsoon index and the geographical distribution of the global monsoons. *Adv. Atmos. Sci.*, **20**, 299–302, doi: 10.1007/s00376-003-0016-5.

Li, Q. P., and Y. H. Ding, 2012: Climate simulation and future projection of precipitation and the water vapor budget in the Haihe River basin. *Acta Meteorologica Sinica*, **26**, 345–361, doi: 10.1007/s13351-012-0307-9.

Li, Z. L., W. Wang, and Z. Li, 2014: Frequency analysis of extremes precipitation in the Heihe River basin based on Generalized Pareto Distribution. *Geographical Research*, **33**, 2169–2179, doi: 10.11821/dlyj201411016. (in Chinese with English abstract)

Liu, W., S. Cao, H. Y. Xi, and Q. Feng, 2010a: Land use history and status of land desertification in the Heihe River Basin. *Natural Hazards*, **53**, 273–290, doi: 10.1007/s11069-009-9429-5.

Liu, Y., J. Y. Sun, H. M. Song, Q. F. Cai, G. Bao, and X. X. Li, 2010b: Tree-ring hydrologic reconstructions for the Heihe River watershed, western China since AD 1430. *Water Research*, **44**, 2781–2792, doi: 10.1016/j.watres.2010.02.013.

Liu, Y. M., and G. X. Wu, 2004: Progress in the study on the formation of the summertime subtropical anticyclone. *Adv. Atmos. Sci.*, **21**, 322–342, doi: 10.1007/BF02915562.

Loarie, S. R., P. B. Duffy, H. Hamilton, G. P. Asner, C. B. Field, and D. D. Ackerly, 2009: The velocity of climate change. *Nature*, **462**, 1052–1055, doi: 10.1038/nature08649.

Lu, L., X. Li, and G. D. Cheng, 2003: Landscape evolution in the middle Heihe River Basin of north-west China during the last decade. *Journal of Arid Environments*, **53**, 395–408, doi: 10.1006/jare.2002.1032.

Ma, M. G., and V. Frank, 2006: Interannual variability of vegetation cover in the Chinese Heihe River basin and its relation to meteorological parameters. *Int. J. Remote Sens.*, **27**, 3473–3486, doi: 10.1080/01431160600593031.

Mann, H. B., 1945: Nonparametric tests against trend. *Econometrica*, **13**, 245–259.

Manton, M. J., and Coauthors, 2001: Trends in extreme daily rainfall and temperature in southeast Asia and the South Pacific: 1961–1998. Int. *J. Climatol.*, **21**, 269–284, doi: 10.1002/joc.610.

Marengo, J. A., J. Tomasella, W. R. Soares, L. M. Alves, and C. A. Nobre, 2012: Extreme climatic events in the Amazon basin. *Theor. Appl. Chimatol.*, **107**, 73–85, doi: 10.1007/s00704-011-0465-1.

Nandintsetseg, B., J. S. Greene, and C. E. Goulden, 2007: Trends in extreme daily precipitation and temperature near Lake Hövsgöl, Mongolia. *Int. J. Climatol.*, **27**, 341–347, doi: 10.1002/joc.1404.

Pal, I., and A. Al-Tabbaa, 2011: Monsoon rainfall extreme indices and tendencies from 1954–2003 in Kerala, India. *Climatic Change*, **106**, 407–419, doi: 10.1007/s10584-011-0044-6.

Peterson, T. C., X. Zhang, M. Brunet-India, and J. L. Vázquez-Aguirre, 2008: Changes in North American extremes derived from daily weather data. *J. Geophys. Res.*, **113**, 1–9, doi: 10.1029/2007JD009453.

Piccarreta, M., A. Pasini, and D. Capolongo, 2013: Changes in daily precipitation extremes in the Mediterranean from 1951 to 2010: The Basilicata region, southern Italy. *Int. J. Climatol*, **33**, 3229–3248, doi: 10.1002/joc.3670.

Qi, S. Z., and F. Luo, 2005: Water environmental degradation of the Heihe River basin arid northwestern China. *Environmental Monitoring and Assessment*, **108**, 205–215, doi: 10.1007/s10661-005-3912-6.

Qi, S. Z., and F. Luo, 2006: Land-use change and its environmental impact in the Heihe River basin, arid northwestern China. *Environmental Geology*, **50**, 535–540, doi: 10.1007/s00254-006-0230-4.

Qin, C., B. Yang, I. Burchardt, X. L. Hu, and X. C. Kang, 2010: Intensified pluvial conditions during the twentieth century in the inland Heihe River basin in arid northwestern China over the past millennium. *Global and Planetary Change*, **72**, 192–200, doi: 10.1016/j.gloplacha.2010.04.005.

R Core Team, 2013: R: A language and environment for statistical computing. R Foundation for Statistical Computing: Vienna, Austria. ISBN 3-900051-07-0. [Available online at: http://www.R-project.org.]

Rajczak, J., P. Pall, and C. Schär, 2013: Projections of extreme precipitation events in regional climate simulations for Europe and the Alpine Region. *J. Geophys. Res.*, **118**, 610–3626, doi: 10.1002/jgrd.50297.

Ran, Q. H., D. Y. Su, P. Li, and Z. G. He, 2012: Experimental study of the impact of rainfall characteristics on runoff generation and soil erosion. *J. Hydrol.*, **424–425**, 99–111, doi: 10.1016/j.jhydrol.2011.12.035.

Rosenberg, E. A., P. W. Keys, D. B. Booth, D. Hartley, J. Burkey, A. C. Steinemann, and D. P. Lettenmaier, 2010: Precipitation extremes and the impacts of climate change on stormwater infrastructure in Washington State. *Climate Change*, **102**, 319–349, doi: 10.1007/s10584-010-9847-0.

Saidi, H., M. Ciampittiello, C. Dresti, and G. Ghiglieri, 2013: Observed variability and trends in extreme rainfall indices and Peaks-Over-Threshold series. *Hydrology and Earth System Sciences Discusses*, **10**, 6049–607, doi: 10.5194/hessd-10-6049-2013.

Sanabria, L. A., and R. P. Cechet, 2010: Severe wind hazard assessment using Monte Carlo simulation. *Environmental Modeling & Assessment*, **15**, 147–154, doi: 10.1007/s10666-008-9188-9.

Samuels, R., A. Rimmer, and P. Alpert, 2009: Effect of extreme rainfall events on the water resources of the Jordan River. *J. Hydrol.*, **375**, 513–523, doi: 10.1016/j.jhydrol.2009.07.001.

Sen, P. K., 1968: Estimates of the regression coefficient based on Kendall's tau. *Journal of the American Statistical Association*, **63**, 1379–1389, doi: 10.1080/01621459.1968.10480934.

Seneviratne, S. I., D. Lüthi, and M. Litschi, 2006: Land-atmosphere coupling and climate change in Europe. *Nature*, **443**, 205–209, doi: 10.1038/nature05095.

Shi, Y. F., Y. P. Shen, E. Kang, D. L. Li, Y. J. Ding, G. W. Zhang, and R. J. Hu, 2007: Recent and future climate change in Northwest China. *J. Climate*, **80**, 379–393, doi: 10.1007/s10584-006-9121-7.

Si, J. H., Q. Feng, X. H. Wen, Y. H. Su, H. Y. Xi, and Z. Q. Chang, 2009: Major ion chemistry of groundwater in the extreme arid region Northwest China. *Environmental Geology*, **57**, 1079–1087, doi: 10.1007/s00254-008-1394-x.

Sillmann, J., V. V. Kharin, X. Zhang, F. W. Zwiers, and D. Bronaugh, 2013a: Climate extremes indices in the CMIP5 multimodel ensemble: Part 1. Model evaluation in the present climate. *J. Geophys. Res.*, **118**, 1716–1733, doi: 10.1002/jgrd.50203.

Sillmann, J., V. V. Kharin, F. W. Zwiers, X. Zhang, and D. Bronaugh, 2013b: Climate extreme indices in the CMIP5 multimodel ensemble: Part 2. Future climate projections. *J. Geophys. Res.*, **118**, 2473–2493, doi: 10.1002/jgrd.50188.

Tang, M. C., 1985: The distribution of precipitation in Mountain Qilian (Nanshan). *Acta Geographica Sinica*, **40**, 323–332.

Trenberth, K. E., A. Dai, R. M. Rasmussen, and D. B. Parsons, 2003: The changing character of precipitation. *Bull. Amer. Meteor. Soc.*, **84**, 1205–1217, doi: 10.1175/BAMS-84-9-1205.

van den Besselaar, E. J. M., A. M. G. Klein Tank, and T. A. Buishand, 2013: Trends in European precipitation extremes over 1951–2010. *Int. J. Climatol.*, **33**, 2682–2689, doi: 10.1002/joc.3619.

van Pelt, S. C., J. J. Beersma, T. A. Buishand, B. J. J. M. van den Hurk, and P. Kabat, 2012: Future changes in extreme precipitation in the Rhine basin based on global and regional climate model simulations. *Hydrology and Earth System Sciences*, **16**, 4517–4530, doi: 10.5194/hess-16-4517-2012.

Vavrus, S. J., and R. J. Behnke, 2013: A comparison of projected future precipitation in Wisconsin using global and downscaled climate model simulations: Implications for public health. *Int. J. Climatol.*, **34**, 3106–3124, doi: 10.1002/joc.3897.

Vincent, L. A., and Coauthors, 2011: Observed trends in indices of daily and extreme temperature and precipitation for the countries of the western Indian Ocean, 1961-2008. *J. Geophys. Res.*, **116**, 1–12, doi: 10.1029/2010JD015303.

Wang, G. X., J. Q. Liu, J. Kubota, and L. Chen, 2007: Effects of land-use changes on hydrological processes in the middle basin of the Heihe River, Northwest China. *Hydrological Processes*, **21**, 1370–1382, doi: 10.1002/hyp.6308.

Wang, H. J., Y. N. Chen, and Z. S. Chen, 2012: Spatial distribution and temporal trends of mean precipitation and extremes in the arid region, northwest of China, during 1960–2010. *Hydrological Processes*, **27**, 1807–1818, doi: 10.1002/hyp.9339.

Wang, H. J., Y. N. Chen, S. Xun, D. M. Lai, Y. T. Fan, and Z. Li, 2013: Changes in daily climate extremes in the arid area of northwestern China. *Theor. Appl. Climatol.*, **112**, 15–28, doi: 10.1007/s00704-012-0698-7.

Wang, J. F., and X. B. Zhang, 2008: Downscaling and projection of winter extreme daily precipitation over North America. *J. Climate*, **21**, 923–937, doi: 10.1175/2007JCLI1671.1.

Wang, J., H. Li, and X. Hao, 2010: Responses of snowmelt runoff to climatic change in an inland river basin, Northwestern China, over the past 50 years. *Hydrology and Earth System Sciences*, **14**, 1979–1987, doi: 10.5194/hess-14-1979-2010.

Wang, K. L., G. D. Cheng, H. L. Xiao, and H. Jiang, 2004: The westerly fluctuation and water vapor transport over the Qilian-Heihe valley. *Science in China Series* (*D*), **47**, 32–38, doi: 10.1360/04yd0004.

Wang, L. M., Q. L. Zhang, and J. Y. Yin, 2003: Study on the growth pattern and bio-productivity of the *Populus Euphratica* forest stand in Ejina. *Journal of Arid Land Resources and Environment*, **17**, 94–99. (in Chinese with English abstract)

Wang, X., and Y. Feng, 2010: RHtestsV3 User Manual, 27 pp. [Available online at: http://etccdi.pacificclimate.org/software.shtml]

Wang, Y. B., Q. Feng, J. H. Si, Y. H. Su, Z. Q. Chang, and H. Y. Xi, 2011: The changes of vegetation cover in Ejina Oasis based on water resources redistribution in Heihe River. *Environmental Earth Sciences*, **64**, 1965–1973, doi: 10.1007/s12665-011-1013-0.

Wang, Y. Q., and L. Zhou, 2005: Observed trends in extreme precipitation events in China during 1961–2001 and the associated changes in large-scale circulation. *Geophys. Res. Lett.*, **32**, L09707, doi: 10.1029/2005GL022574.

Wen, L. J., and J. M. Jin, 2012: Modelling and analysis of the impact of irrigation on local arid climate over Northwest China. *Hydrological Processes*, **26**, 445–453, doi: 10.1002/hyp.8142.

Williams, C. J. R., and D. R. Kniveton, 2012: Atmosphere-land surface interactions and their influence on extreme rainfall and potential abrupt climate change over southern Africa. *Climate Change*, **112**, 981–996, doi: 10.1007/s10584-011-0266-7.

Xie, Y. W., L. L. Li, X. J. Zhao, and C. X. Yuan, 2012: Temporal-spatial changes of the oasis in the Heihe River basin over the past 25 years. Sustainable development-education, business and management-architecture and building construction-agriculture and food security. G. Chaouki, Ed., InTech, Croatia, 313–330.

Xu, J. W., and Y. H. Gao, 2014: Validation of summer surface air temperature and precipitation simulation over Heihe River basin. *Plateau Meteorology*, **33**, 937–946. (in Chinese with English abstract)

Yin, Y. Y., 2006: Vulnerability and adaptation to climate variability and change in western China. AIACC, Project No. AS 25, 106 pp.

You, Q. L., and Coauthors, 2011: Changes in daily climate extremes in China and their connection to the large scale atmospheric circulation during 1961–2003. *Climate Dyn.*, **36**, 2399–2417, doi: 10.1007/s00382-009-0735-0.

Yu, R. C., B. Wang, and T. J. Zhou, 2004: Tropospheric cooling and summer monsoon weakening trend over East Asia. *Geophys. Res. Lett.*, **31**, 1–4, doi: 10.1029/2004GL021270.

Yue, S., P. Pilon, B. Phinney, and G. Cavadias, 2002: The influence of autocorrelation on the ability to detect trend in hydrological series. *Hydrological Processes*, **16**, 1807–1829, doi: 10.1002/hyp.1095.

Zhai, P. M., X. B. Zhang, H. Wan, and X. H. Pan, 2005: Trends in total precipitation and frequency of daily precipitation extremes over China. *J. Climate*, **18**, 1096–1108, doi: 10.1175/JCLI-3318.1.

Zhang, A. J., C. M. Zheng, S. Wang, and Y. Y. Yao, 2015: Analysis of streamflow variations in the Heihe River basin, Northwest China: trends, abrupt changes, driving factors and ecological influences. *J. Hydrol.*, **3**, 106–124, doi: 10.1016/j.ejrh.2014.10.005.

Zhang, J. S., E. S. Kang, Y. C. Lan, and R. S. Chen, 2003: Impact of climate change and variability on water resources in Heihe River basin. *Journal of Geographical Sciences*, **13**, 286–292, doi: 10.1007/BF02837501.

Zhang, Q., J. F. Li, V. P. Singh, and C. Y. Xu, 2003: Copula-based spatio-temporal patterns of precipitation extremes in China. *Int. J. Climatol.*, **33**, 1140–1152, doi: 10.1002/joc.3499.

Zhang, Q., V. P. Singh, J. F. Li, and X. H. Chen, 2011a: Analysis of the periods of maximum consecutive wet days in China. *J. Geophys. Res.*, **116**, 1–18, doi: 10.1029/2011JD016088.

Zhang, Q., C. Y. Xu, Z. X. Zhang, and Y. D. Chen, 2010: Changes of atmospheric water vapor budget in the Pearl River basin and possible implications for hydrological cycle. *Theor. Appl. Climatol.*, **102**, 185–195, doi: 10.1007/s00704-010-0257-z.

Zhang, X. B., L. V. Alexander, G. C. Hegerl, P. Jones, A. K. Tank, T. C. Peterson, B. Trewin, and F. W. Zwiers, 2011b: Indices for monitoring changes in extremes based on daily temperature and precipitation data. *Wiley Interdisciplinary Reviews: Climate Change*, **2**, 851–870, doi: 10.1002/wcc.147.

Zhao, C., Z. Nan, and G. Cheng, 2005: Methods for estimating irrigation needs of spring wheat in the middle Heihe basin, China. *Agricultural Water Management*, **75**, 54–70, doi: 10.1016/j.agwat.2004.12.003.

Zhao, W. Z., B. Liu, and Z. H. Zhang, 2010: Water requirements of maize in the middle Heihe River basin, China. *Agricultural Water Management*, **97**, 215–223, doi: 10.1016/j.agwat.2009.09.011.

Zhou, T. J., and Coauthors, 2009: Why the western Pacific subtropical high has extended westward since the Late 1970s. *J. Climate*, **22**, 2199–2215, doi: 10.1175/2008JCLI2527.1.